Diffusion mechanics of the system PMMA–methanol

N. L. Thomas* **and A. H. Windle**
Department of Metallurgy and Materials Science, University of Cambridge, Pembroke Street, Cambridge, UK
(*Received* 14 *August* 1980; *revised* 10 *October* 1980)

Case II diffusion of penetrants in polymer sheet is associated with constrained swelling of the material and the generation of internal stresses. The work reported here is based on data from the model system PMMA–methanol. Specimen dimensions have been measured during swelling and these are related to the mechanics of the diffusion process. In particular the discontinuous reduction in sheet specimen thickness when the fronts meet has been compared with behaviour predicted from a simple model of Case II diffusion. The fact that there is a quantitative discrepancy indicates that the specimen shape change, as the fronts meet, is also accompanied by an increase in the degree of 'equilibrium' solvent uptake as the hydrostatic stress component on the swollen layers is relaxed. This increase is accounted for in terms of thermodynamic equations incorporating the work of deformation of a rubber network and it is apparent that a measurement of the volume change in a swelling polymer, when approaching Case II fronts meet, can give a measure of the Flory–Huggins interaction parameter χ. At elevated temperatures a substantial concentration gradient develops behind the advancing fronts, which complicates the prediction of the discontinuous shape change observed at 42°C, 52°C and 62°C. The generation and partial relaxation of molecular orientations behind the advancing Case II fronts has been observed by optical birefringence. The technique has also been used to study the development of biaxial tensile stresses in the surface layers during desorption of partially swollen specimens. These stresses readily exceed that necessary for crazing, and a sorption–desorption cycle has been shown to induce such mechanical damage in the absence of any external or prior internal stress.

INTRODUCTION

When a sample of polymer is immersed in an organic liquid, solvent molecules will diffuse into the solid polymer to produce a swollen gel. Dissolution is prevented if the attraction between neighbouring polymer molecules is sufficiently great—perhaps due to crosslinking or hydrogen bonding. Swelling continues until the elastic reaction of the network balances the osmotic pressure driving the solvent into the swollen polymer.

Elasticity theory has been used to explain the swelling behaviour of rubbery systems with considerable success[1–3]. However, in glassy systems swelling is more complicated because the expansion required to accommodate the imbibed penetrant is at first restrained by the unpenetrated glassy material. Because of the inability of the glassy core to extend, compressive stresses are set up along the plane of the specimen surface and initial swelling will occur mainly perpendicular to the surface giving a marked thickness increase. For example, Dreschel *et al.*[4] have observed anisotropic swelling of cellulose nitrate films in acetone and Park[5] has reported similar effects when polystyrene sheets are immersed in methylene chloride.

The processes of both diffusion and swelling are more complicated in glassy, than in rubbery systems. Well above T_g, organic penetrants diffuse into polymer networks in accordance with Fick's laws. However, in the glassy state, time-dependent structural rearrangements give rise to deviations from Fickian behaviour. The complex diffusion behaviour of organic penetrants in glassy polymers (known as 'anomalous' diffusion) may be simplified by considering 'relaxation-controlled' transport as a second simple limiting type of diffusion behaviour in these systems. Relaxation-controlled or Case II transport (as opposed to Case I, i.e. Fickian diffusion) was first proposed by Alfrey *et al.*[6] and describes diffusion behaviour in which penetrant transport is completely controlled by the relaxation rate of chain segments in the glassy polymer. Case II transport is characterized by a sharp front moving into the polymer at constant velocity. This sharp boundary separates an outer swollen shell, essentially at equilibrium penetrant concentration, from an unpenetrated glassy core. The mass of penetrant absorbed therefore, increases linearly with time (as in *Figure 1*). Case II transport has been reported in a variety of systems[7–10].

A sharp boundary separating the swollen and unpenetrated material is often observed when a polymer sample is immersed in an organic penetrant—although the existence of a sharp front *per se* is not a sufficient condition for Case II transport[8,11,12]. Surface compression in the swollen gel will be balanced by biaxial tension in the unpenetrated core of the specimen and a steep stress gradient can be expected at the front. These internal stresses tend to extend the glassy core and increase the area of the sheet. Direct evidence for the existence of such internal stresses has been reported in several systems. For example, Hermans[13] has reported pronounced transverse fracturing of the dry inner core during swelling of cellulose filaments. On swelling Novalac (phenol formaldehyde resin) films in water, Rosen[14] observed cracking due to

* Now at Dept. of Metallurgy and Materials Science, University of Oxford, Parks Road, Oxford.

0032-3861/81/050627-13$02.00
© 1981 IPC Business Press

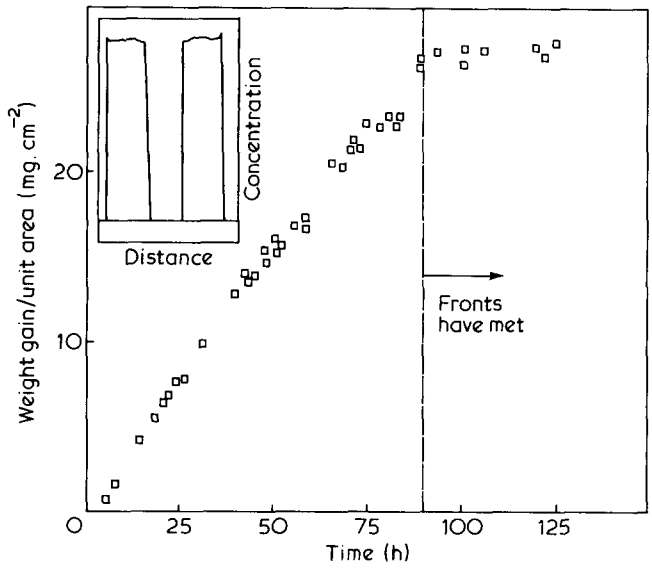

Figure 1 Weight gain/unit area *versus* time at 24°C for 1 mm sheet PMMA specimens swollen in methanol at 24°C, with inset of typical concentration profile

biaxial tensile stresses on both absorption and desorption.

Alfrey *et al.*[6] have considered the effect of stresses accompanying Case II penetration in glassy polymers. The theory is an attempt to predict the stress distribution in a partially swollen specimen, from a consideration of the elastic force necessary to bring the hypothetical unconstrained swollen gel back into contact with the glassy core. The model predicts that the tensile core stresses increase continuously as the swelling fronts advance inward, and become infinitely large as the Case II fronts meet in the centre of the specimen. This implies that the core stress is bound to reach the tensile strength of the glassy polymer and fracture should occur ahead of a Case II front in every case, which is clearly not true. However, the model does successfully account for the transverse core fractures observed during the swelling of cylindrical specimens because it predicts that the axial tension is the largest in the cylindrical core.

The cases of solvent cracking during absorption cited above were all explained in terms of crack (or craze) initiation due to tensile stresses in the glassy core ahead of the penetrating solvent front. However, Michaels *et al.*[15] found that treatment of both biaxially oriented polystyrene and cast, annealed polystyrene with n-heptane resulted in a 'sandwich structure' of expanded, crazed outer layers surrounding an apparently unaffected central core. Void formation was attributed to 'localized swelling-fracture' of the polymer and crazes were thought to be initiated at or just behind the penetrating Case II front. The craze initiation stress is therefore not the tensile reaction stress in the core ahead of the front, but presumably is a local swelling stress (tensile or shear) at the front.

Hopfenberg *et al.*[16] have suggested that solvent crazing and some forms of environmental stress cracking are a simple extension of Case II transport and that crazing should accompany Case II sorption processes if sufficiently large swelling stresses are generated at the boundary between swollen and unswollen polymer.

In this paper we present observations on the system PMMA–methanol. They include anisotropic dimension changes of the sample, the effect of constraint on the equilibrium absorption in swollen surface layers, the development of birefringence and the occurrence of crazing during swelling and desorption experiments. These phenomena are all the result of internal stresses generated during the swelling and desorption processes and as such their investigation is essential to the understanding of diffusion in such a system.

EXPERIMENTAL OBSERVATIONS OF SHAPE CHANGE

Changes in thickness and area were measured as thin sheets of PMMA (ICI 'Perspex') were swollen in methanol at temperatures in the range from 15 to 62°C. The specimens, of major surface dimensions 40 × 20 mm, were cut from a 1 mm (nominal) sheet and subsequently pre-annealed for 1 h at 130°C and cooled through T_g at 1.3°C min^{-1}. This pre-treatment was chosen to try and minimize the effects of subsequent shape relaxation without causing degradation of the polymer. It caused a 3.0% thickness increase with a corresponding reduction in specimen area, although a later examination showed that with a longer annealing time and slower cooling rate a further $0.5 \pm 0.2\%$ thickness increase could be achieved.

The measurements were made by micrometer on the sheet samples immediately (< 5 s) on removal from the methanol. Once a sample had been measured it was not re-immersed and re-used. Each data point represents a fresh sample.

Earlier detailed studies[8,17] of the transport kinetics of liquid methanol in PMMA sheet made from 0° to 62°C have revealed that at ambient temperatures and below, the behaviour is typical of Case II transport, but as the temperature is raised the diffusion process becomes increasingly Fickian in character.

Swelling behaviour in the Case II regime will be considered first.

Data at ambient temperature

Specimens were found to change shape during swelling. *Figure 2* shows increases in specimen thickness and area as a function of swelling time at 24°C. Thickness increases linearly with time until the sharp Case II fronts (separating the outer swollen gel from the unpenetrated core) meet at the centre of the specimen. At this point there has been a thickness increase of 23%. There is then a discontinuity in the plot representing a decrease in thickness, which continues until an 'equilibrium' value of $9.0 \pm 0.2\%$ (total increase) is reached. Note, however, that the data are plotted in absolute units and not percentages. In this way scatter, due to variations in the original sheet thickness between samples, is minimized, although at the expense of possible scatter in the exact position (in time) of the discontinuity on such a plot.

Specimen area increases only slightly before the fronts meet (it has changed) by merely 2% at this stage, and this increase can be entirely accounted for in terms of the swelling of the specimen edges. After the fronts have met, however, the specimen area undergoes a rapid increase (corresponding to the decrease in thickness) and continues to do so until an equilibrium value of $17.5 \pm 0.2\%$ is reached. The equilibrium values quoted were measured 400 h after the start of the experiment.

If the specimens return exactly to their original shape, the relationship between the fractional area increase ($\Delta A/A_0$) and the fractional thickness increase ($\Delta A/t_0$) is:

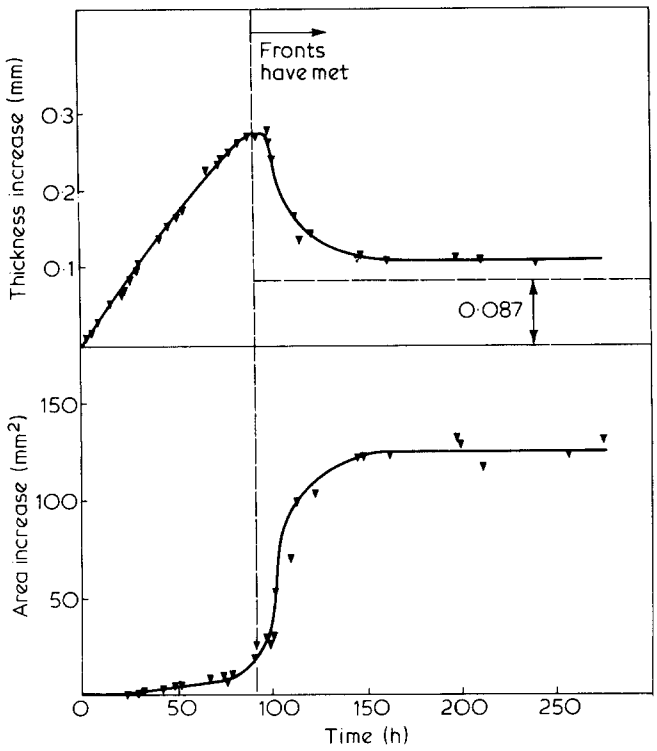

Figure 2 Thickness and area increase as a function of time on swelling 1 mm (nominal thickness) specimens at 24° C. (Actual initial thickness is 1.18 mm)

$$\frac{\Delta A}{A_0} = \frac{2\Delta t}{t_0} + \left(\frac{\Delta t}{t_0}\right)^2 \qquad (1)$$

Given that the specimens used had not quite reached their equilibrium shape before swelling, i.e. the thickness was $0.5 \pm 0.2\%$ less than the equilibrium value and the area correspondingly greater, the true equilibrium values of $\Delta t/t_0$ and $\Delta A/A_0$ were $8.5 \pm 0.4\%$ and $18.5 \pm 0.4\%$. Hence equation 1 is satisfied showing that the original shape is entirely restored at long time periods, i.e. at 24°C the swollen polymer deforms as a rubber.

These observations of shape change can be explained in terms of the constraint imposed on the specimen by the unswollen glassy core. A small element of glassy polymer just ahead of the front becomes swollen as the sharp front moves forward and penetrant molecules enter the element under the driving force of the osmotic swelling stress. Isotropic volume expansion of this element is prevented by the constraint of the glass ahead of it, and so to increase in volume the element must change its shape. Hence (ignoring edge effects) all volume change appears as increase in thickness. When the fronts meet, the constraint of the glassy core is lost and the specimen can relax back to its original shape. Note, however, that the shape change does not begin to reverse until about 10 h after the fronts have met, and then the specimen relaxes slowly back to its initial state. The elastic behaviour is retarded because the swollen 'rubber' is only just above its T_g.

*Figure 3** shows thickness increase as a function of time for specimens swollen at 15°C. The Case II fronts meet after 15 days when there has been a thickness increase of 23%, however, after a further 45 days the total increase in thickness has only reduced to 21.5%. Shape reversion is greatly retarded in this case indicating that the swollen gel is below its effective T_g.

* *Figure 9* of reference 17

Analysis of Case II data

Figure 4(a) is a schematic representation of the swelling process. A cubic element of polymer of original dimensions t_0 is swollen unidirectionally to a length t. The ratio t_0/t is then equivalent to the volume fraction of polymer, v_2. If the element subsequently relaxes at constant volume to its original shape, the edge lengths of the cube, t', will be given by the relation:

$$t' = (tt_0^2)^{1/3} \qquad (2)$$

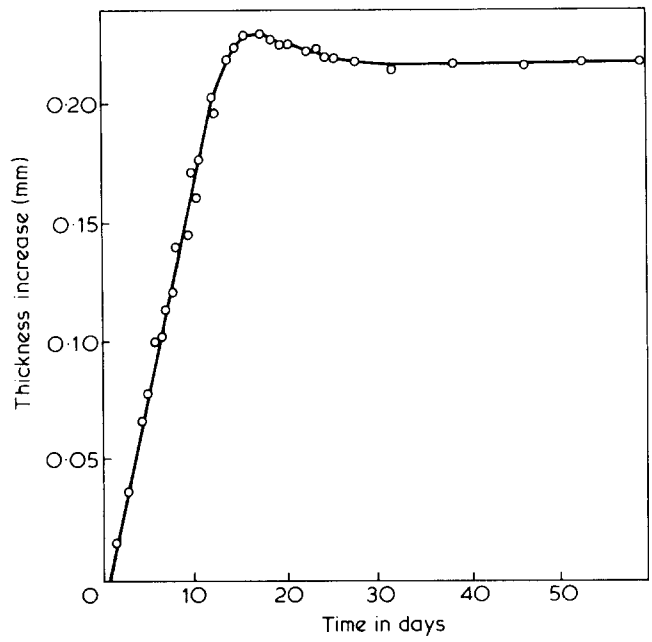

Figure 3 Thickness increase as a function of time at 15°C. (Initial thickness is 1.00 mm)

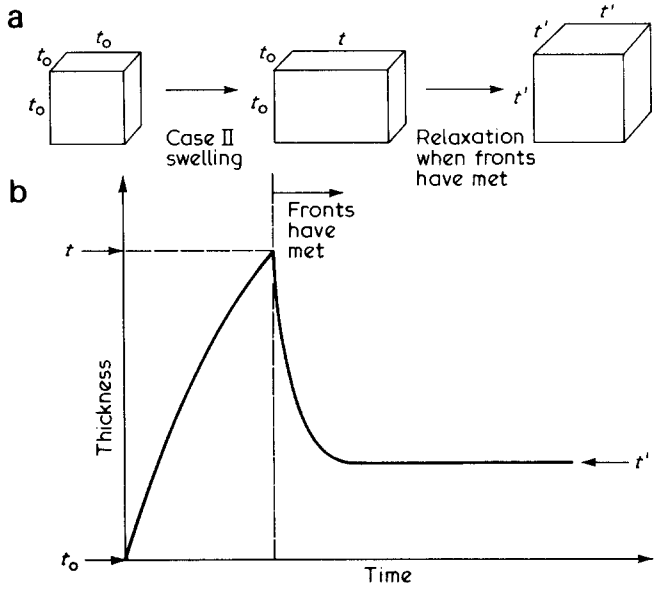

Figure 4(a) Schematic representation of the anisotropic swelling and subsequent relaxation of a cubic element of polymer. (*b*) Schematic plot of thickness increase as a function of time for Case II swelling, when the swollen gel is just above T_g

Hence the shape change on relaxation expressed as an extension ratio with respect to the relaxed state, t/t', is given by:

$$t/t' = (t/t_0)^{2/3} \tag{3}$$

It is possible to measure the three parameters, t_0, t and t' from the thickness data (shown schematically in *Figure 4(b)*). For the sample swollen at 24°C they have values of 1.18 mm, 1.46 mm and 1.29 mm respectively and should, if the model properly describes the phenomenon, be related by equations 2 and 3. Substitution of the measured values of t_0 and t into equation 2 gives a calculated value of t' of 1.267, (t'_{calc}) compared with the measured value of 1.29 mm (t'_{exp}). Putting this another way, the measured values of t_0 and t would predict, on the basis of the geometric equation 2, that the overall thickness increase after relaxation would be 0.087 mm which is less than that observed. The comparison is made with the experimental data on *Figure 2*. The most straightforward explanation of this discrepancy is that the relaxation process is accompanied by an increase in volume of the sample. This is equivalent to saying that the equilibrium swelling (for Case II) of the constrained rubbery material is less than that for the fully penetrated, relaxed specimen. The amount of additional swelling on relaxation can be expressed by the volume ratio of $(t'_{exp})^3/(t'_{calc})^3$, which for our sample is a volume increase of 5.4%.

It appears that at 24°C the volume change associated with the readjustment of methanol content can occur quickly during the relatively slow shape change reversion process.

Influence of shape constraint on equilibrium swelling

The effect of shape constraint on swelling behaviour is analogous to the problem of the mechanical deformation of swollen networks first treated by Flory and Rehner in 1944[18] and since modified in keeping with developments in the theory of rubber elasticity[19,20].

The swelling of the constrained polymer in Case II sorption produces a change in shape which amounts to a tensile strain normal to the surface at effectively zero Poisson's ratio. That is if we assume complete area constraint. This situation stands out from the various practical cases treated by Treloar[1] in that no external work is done on or by the specimen (neglecting expansion against atmospheric pressure).

Following the argument of Hermans[21] as discussed in reference 3, and more recently supported by Flory for perfect networks of functionality for[22] the Helmholtz free energy in terms of the strain ratios λ_x, λ_y and λ_z is given by:

$$\Delta A = \frac{GkT}{2}[\eta(\lambda_x^2+\lambda_y^2+\lambda_z^2)-3] - GkT\ \ln(\eta^{3/2}\lambda_x\lambda_y\lambda_z) \tag{4}$$

Where η is the Tobolsky front factor which takes into account changes in conformational energy. It is here assumed to be unity. G is the number of network segments in the unswollen polymer, k, Boltzmann's constant and T absolute temperature.

Combination of this equation with that suggested by Flory and Huggins, which describes the free energy of mixing, gives for isotropic swelling where the volume fraction of polymer $v_2 = \dfrac{1}{\lambda_1\lambda_2\lambda_3}$:

$$\Delta F = kT\left[\frac{3G}{2}(v_2^{-2/3}-1) - G\ln v_2^{-1} + N_i\ln(1-v_2) + \chi N_i v_2\right] \tag{5}$$

(N_i is the number of diluent molecules and χ the polymer–liquid interaction parameter).

Working this relation in accord with reference 3 p.373 gives the condition for equilibrium isotropic swelling as:

$$\frac{G\bar{V}_1}{V_i}[v_2^{1/3}-v_2] + \ln(1-v_2) + v_2 + \chi v_2^2 = 0 \tag{6}$$

This is an established result, and $\bar{V}_1$ is the molecular volume of the diluent and V_i is the volume of the unswollen polymer. It is also interesting to note that the derivation is based on a definition of v_2 (i.e. v = Volume of polymer/Volume of swollen polymer) which is not quite the same as that more generally used (i.e. v = Volume of polymer/Volume of polymer + volume of liquid).

Where the polymer is constrained such that $\lambda_2 = \lambda_3 = 1$, v_2 is now equal to $1/\lambda_1$.

Equation 4 for ΔA becomes:

$$\Delta A = \frac{GkT}{2}[\lambda_1^2 - 1] - GkT\ \ln(\lambda_1) \tag{7}$$

which because of the relation:

$$\frac{1}{v_2} = \lambda_1\lambda_2\lambda_3 = \left(\frac{N_i\bar{V}_1}{V_i}+1\right) \tag{8}$$

gives on differentiation:

$$\begin{aligned}\left(\frac{dA}{dN}\right) &= \left(\frac{dA}{d\lambda_1}\right)_{\lambda_2\lambda_3}\cdot\left(\frac{d\lambda_1}{dN}\right)\\ &= \left(GkT\left[\lambda_1 - \frac{1}{\lambda_1}\right]\right)\left(\frac{\bar{V}_1}{V_i}\right)\\ &= \frac{GkT\,\bar{V}_1}{V_i}\left(\frac{1}{v_2'} - v_2'\right)\end{aligned} \tag{9}$$

(where v_2' designates the equilibrium volume fraction of polymer for constrained swelling).

Thus combining this with the differential of the Flory–Huggins component of the free energy we have:

$$\frac{dA}{dN} = kT\left[\frac{G\bar{V}_1}{V_i}\left(\frac{1}{v_2'} - v_2'\right) + \ln(1-v_2') + v_2' + \chi v_2'^2\right]$$

Because for this constrained situation the polymer is incapable of doing external work, this relation may be equated directly with $(d\Delta F/dN)$ and put equal to zero for equilibrium.

Hence for constrained swelling in which $\lambda_2 = \lambda_3 = 1$,

$$\frac{G\bar{V}_1}{V_i}\left(\frac{1}{v_2'} - v_2'\right) + \ln(1-v_2') + v_2' + \chi v_2'^2 = 0 \tag{10}$$

The assumption that the term $G\bar{V}_1/V_i$ is identical for both isotropic and constrained swelling enables 6 and 10 to be combined:

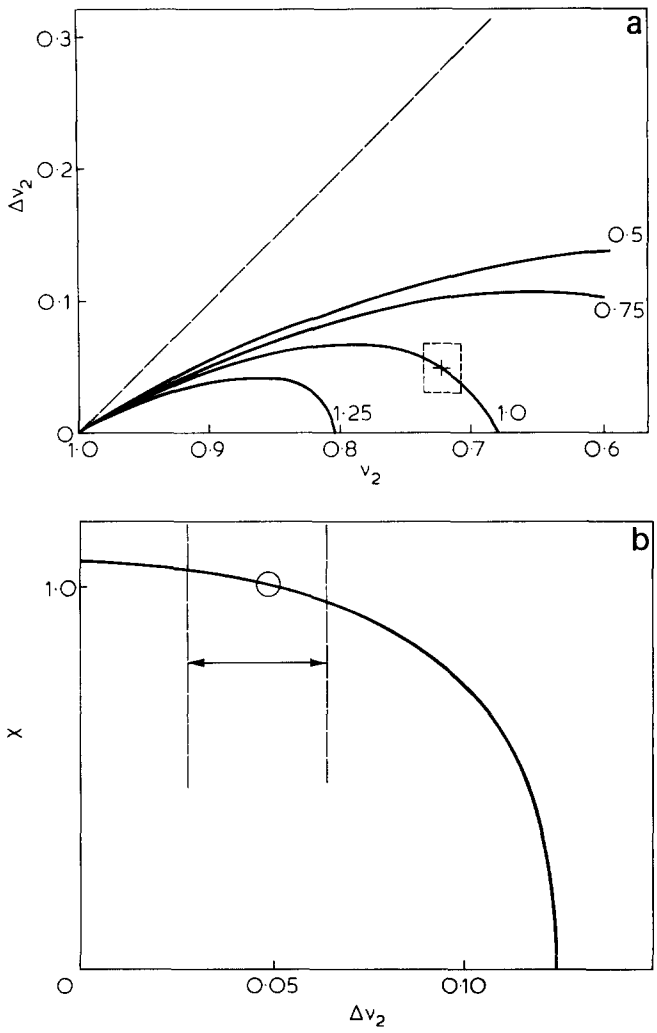

Figure 5(a) Plot of calculated increase in swelling (expressed as the change in polymer volume fraction (Δv_2) which occurs during shape relaxation when the Case II fronts meet) *versus* the equilibrium swelling after relaxation (i.e. polymer volume fraction v_2). The curves are drawn for different values of the Flory–Huggins interaction parameter χ. The experimental point (+) is obtained from measurements of the specimen volume just before and after the fronts meet. (*b*) Calculated plot of χ against Δv_2 at the experimentally observed value of v_2 (= 0.723). The measured range of Δv_2 is indicated on the graph

$$\frac{\ln(1-v_2)+v_2+\chi v_2^{\,2}}{(v_2^{\,1/3}-v_2)}=\frac{\ln(1-v_2')+v_2'+\chi v_2'^{\,2}}{\left(\frac{1}{v_2'}-v_2'\right)} \quad (11)$$

It is thus possible, for given values of the solvent–polymer interaction parameter χ to determine the relationships between v_2 and v_2', i.e. the effect of constraint on equilibrium absorption. Results of such calculations are shown in *Figure 5a*.

Micrometer measurements made on the swelling sample given above yield values of v_2 as follows: At the point at which the fronts meet but before any relaxation: $v_2' = 0.770 \pm 0.004$; fully relaxed: $v_2 = 0.723 \pm 0.014$.

These data are plotted on *Figure 5a* and assigned an 'error box'. They indicate a value of $\chi \simeq 1.00$ for PMMA swollen by methanol at 24°C.

Figure 5(b) is a plot of χ against Δv_2, the change in volume fraction of polymer for the experimentally observed equilibrium swelling of 27.7% ($v_2 = 0.723$). It is apparent that error limits of ± 0.05 are reasonable for the value of $\chi = 1.00$. For smaller values of χ the uncertainty would obviously have been greater.

It is possible to extend these calculations to determine the value of G, the number of chain segments per unit volume. However, the value is not likely to be particularly accurate, for situations such as the example we have considered in which the swelling is not especially large.

This work has demonstrated that, for a polymer–penetrant system in which the diffusion mechanism is Case II, it is possible to determine a value for the thermodynamic interaction parameter χ by micrometer measurements alone. The main limitation on the precision of the method is the uncertainty concerning the exact form of the rubber elasticity equation on which the Flory–Huggins relation is based.

It is interesting to note that a similar approach to the development of equation 10, has been presented by H. R. Brown[23] in his study of environmental stress cracking of polyethylene. He considered the swelling of the interlamellar amorphous regions to be subject to area constraint by the neighbouring crystallites and calculated the influence of applied hydrostatic stress components on the equilibrium swelling for a range of low molecular weight liquids. His analysis, however, is based on Treloar's equations which omit the log-term in equation 4, so that his equivalent to our equation 10 has the first bracketed term reduced to $(1/v_2')$.

The experiment suggests that for any swelling system, whether Case II diffusion is involved or not, it will be possible to determine χ by precise linear measurement if lateral constraint is applied to the swelling specimen by carrying out the experiment with the specimen fitted into a rigid and internally smooth tube. The specimen would then have to be pushed out of the tube to obtain the second equilibrium absorbtion when the swelling is isotropic. However, as with the Case II experiment, meaningful measurements would only be obtained if there was no significant viscous relaxation of the molecular network.

Super Case II diffusion

Jacques, Hopfenberg and Stannett[24], in their study of n-hexane absorption in films of polystyrene, polyphenylene oxide and blends of these two polymers, found marked increases in the rate of sorption, as determined by weight increase, during the final stages of the sorption process. The phenomenon was called 'super' Case II diffusion and was explained in terms of overlapping of the Fickian precursors to the sharp fronts as they approached each other in the centre of the specimen.

The fact that the meeting of the sharp fronts is associated with an adjustment in equilibrium concentration in the swollen specimen, as shown in the previous section, can provide an alternative explanation for super Case II diffusion. *Figure 6* is a schematic sketch of a weight-gain plot for Case II diffusion in which there is a readjustment of equilibrium when the fronts meet and the swollen material undergoes shape relaxation. The adjustment in equilibrium in this situation will always result in an additional increment in the amount absorbed.

The rate at which the new equilibrium is attained once the fronts have met remains a matter for conjecture. It may be more rapid and hence give rise to a steeper gradient than the Case II sorption itself, in which case it will be indistinguishable from 'super' Case II diffusion as

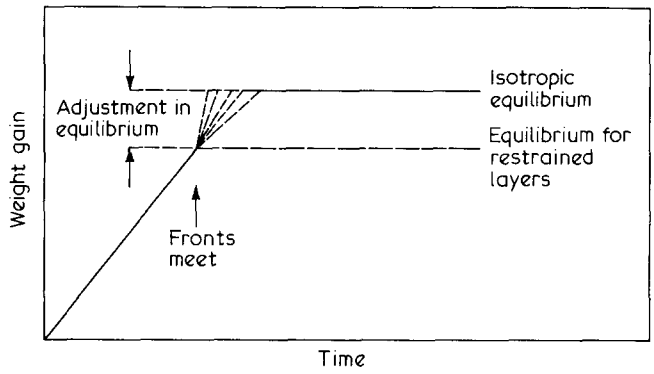

Figure 6 Schematic diagram illustrating how the adjustment in equilibrium volume after the Case II fronts have met might cause a change in slope in the weight gain–time relationship just prior to final equilibrium. The lines joining the two equilibrium weights illustrate possible paths which might occur. The only experimental evidence available suggests that there is an increase in slope. However, there is no reason why this top portion of the plot should be linear

described by Jacques *et al.*[24]. It may be less rapid or indeed equally rapid in which case the effect would not be clearly apparent from the weight gain vs time plot. The 'adjusting' portions of the plot are sketched as linear in *Figure 6*, but there is no real reason why they should be.

The weight gain data obtained at 24°C (*Figure 1*) have too much scatter to confirm any change of slope as absorption is completed. However, there does appear to be a suggestive discontinuity. More precise work is needed in this area.

Super Case II diffusion, for the systems studied by Jacques *et al.* would be scarcely apparent in specimens as thick as 1 mm (theirs were less than 0.1 mm), and we would not expect to see it in our system. However, we predict that there will be a readjustment in equilibrium sorption as the fronts meet, which can change the slope of the final stages of the weight gain *versus* time plot. There is strong evidence for this readjustment from measurement of dimension changes and some support from weight-gain plots at various temperatures. Under certain circumstances the effect produced could be referred to as 'super' Case II in its own right, but in any case its presence will complicate the analysis of accelerated absorption associated with overlapping Fickian precursors where this is seen.

SUPERSHAPE CHANGE AT ELEVATED TEMPERATURES

Experimental Data

As the swelling temperature is increased from ambient up to the boiling point of the methanol, departures from Case II kinetics become increasingly significant and the exponent of time describing the methanol uptake approaches 0.5—the value typical of Fickian diffusion. The trend towards Fickian behaviour at the higher temperatures can be explained in terms of concentration gradients in the swollen polymer behind the advancing fronts which are observed to steepen as the temperature is increased[8].

Shape change occurs during swelling. The increases in thickness and area on swelling specimens (40 × 20 × 1 mm) at 42°C, 52°C and 62°C are plotted in *Figures 7*, *8* and *9* respectively, and the concentration profile, as measured just before the fronts meet, is inserted in each case. The profiles were obtained by microdensitometry of thin sections of swollen specimens in which the methanol had been coloured by iodine. The technique is fully described and assessed in reference 8. At these temperatures the swollen gel is considerably above its effective T_g (attained at 20°C with a 21% weight gain) and when the fronts meet the reversal of shape change takes place immediately and there is a sudden decrease in thickness and a corresponding increase in area. As is evident from the concentration profiles, equilibrium sorption is not reached until some time after the fronts have met and so after the shape change reversal the specimens continue to swell until reaching their equilibrium volume.

General description of data

It has been demonstrated that for Case II swelling there is a discrepancy between the fractional volume increase after unidirectional swelling and that achieved when the fronts have met and the specimen has reverted to its original shape. When the Case II fronts meet there is an increase in the swollen volume because the release of the compressive stresses in the swollen network allows further imbition of solvent. This situation should also occur at elevated temperatures.

Figure 10 is a schematic representation of thickness increase as a function of time at elevated temperatures; it

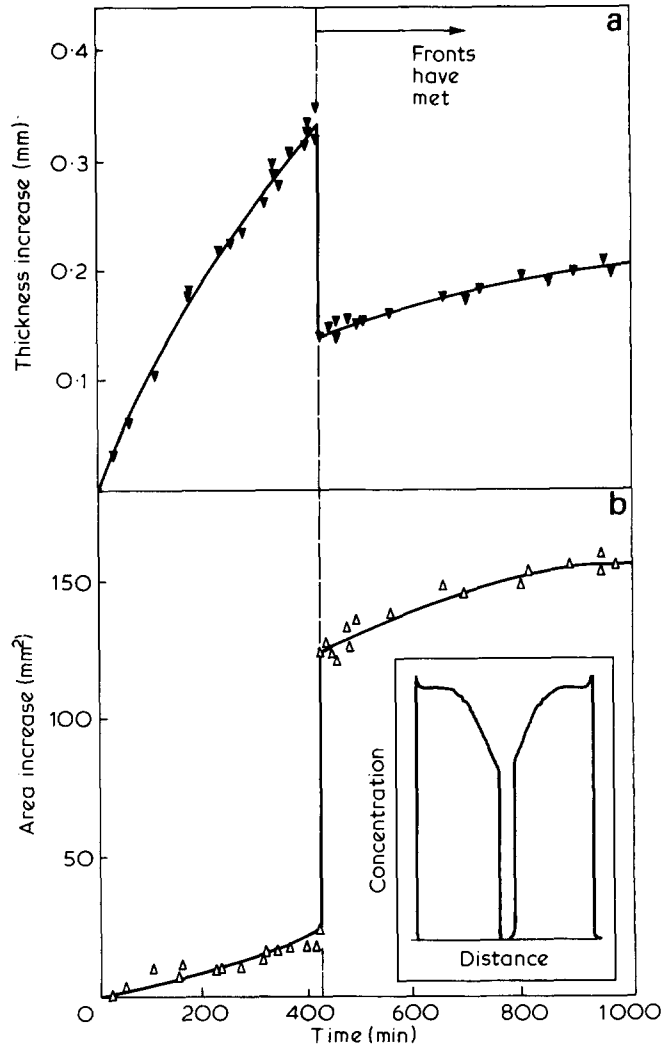

Figure 7 Thickness and area increase as a function of time at 42°C, with inset of concentration profile just before the fronts meet

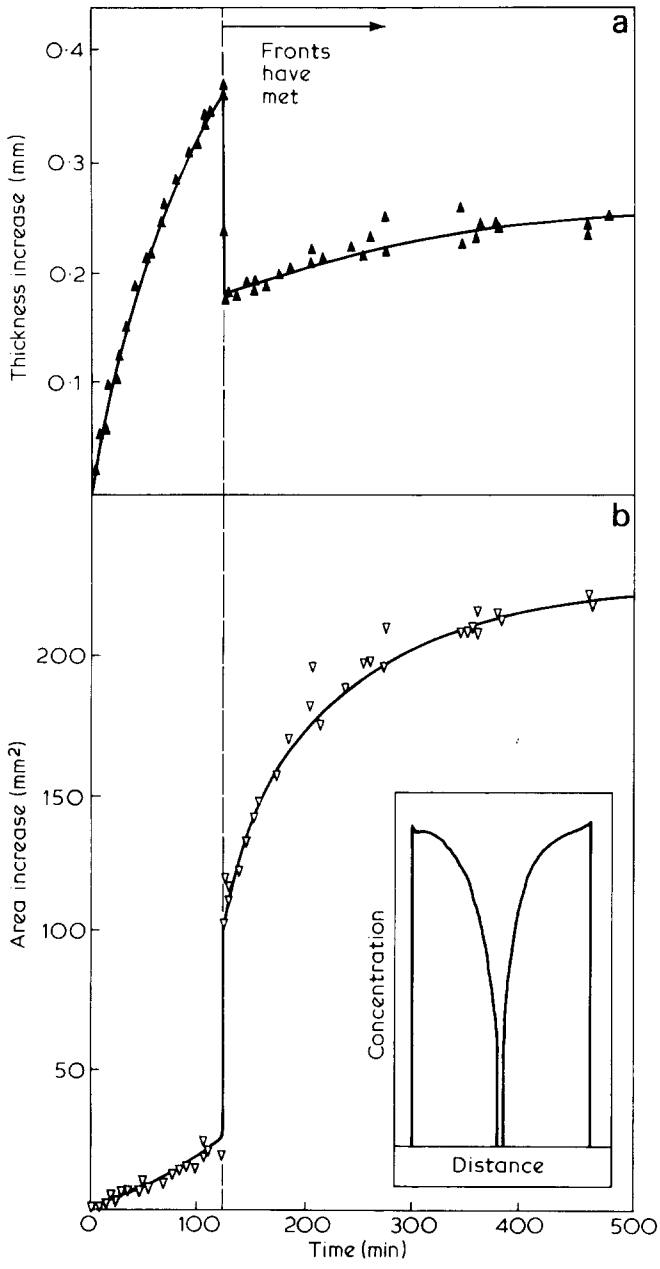

Figure 8 Thickness and area increase as a function of time at 52°C, with inset of concentration profile just before the fronts meet

is also annotated with schematic concentration profiles. Shape reversion occurs immediately when the fronts meet and then further swelling, associated with both the 'filling in' of the profiles and the adjustment to the new equilibrium volume, occurs until a uniform concentration is achieved across the specimen. The parameters, t_0, t and t' are as previously defined and used in equations 2 and 3.

Evidence for an increase in equilibrium volume after shape reversion

The qualitative explanation of the form of *Figure 10* is based on the expectation that a readjustment in equilibrium will occur on shape reversion at elevated temperatures as for the pure Case II situation at room temperature, and that at the higher temperatures the reversion will occur relatively more rapidly than the adjustment of penetrant volume and profiles. Evidence that the readjustment to the new equilibrium concentration does occur over a period after the shape reversion is complete is provided by the data presented in *Figure 11*. The experimental points on the weight gain plots are compared with curves calculated from measured concentration profiles[8] on the assumption that the area under the profile is proportional to the weight gain and that the concentration at the surfaces remains constant at the final equilibrium value. The experimental and derived curves are normalized to give the best fit up to the point at which the fronts meet. Their gradual divergence at longer times is the result of the increased (equilibrium) surface concentration and the consequent changes of the actual profiles as they accommodate to this new value.

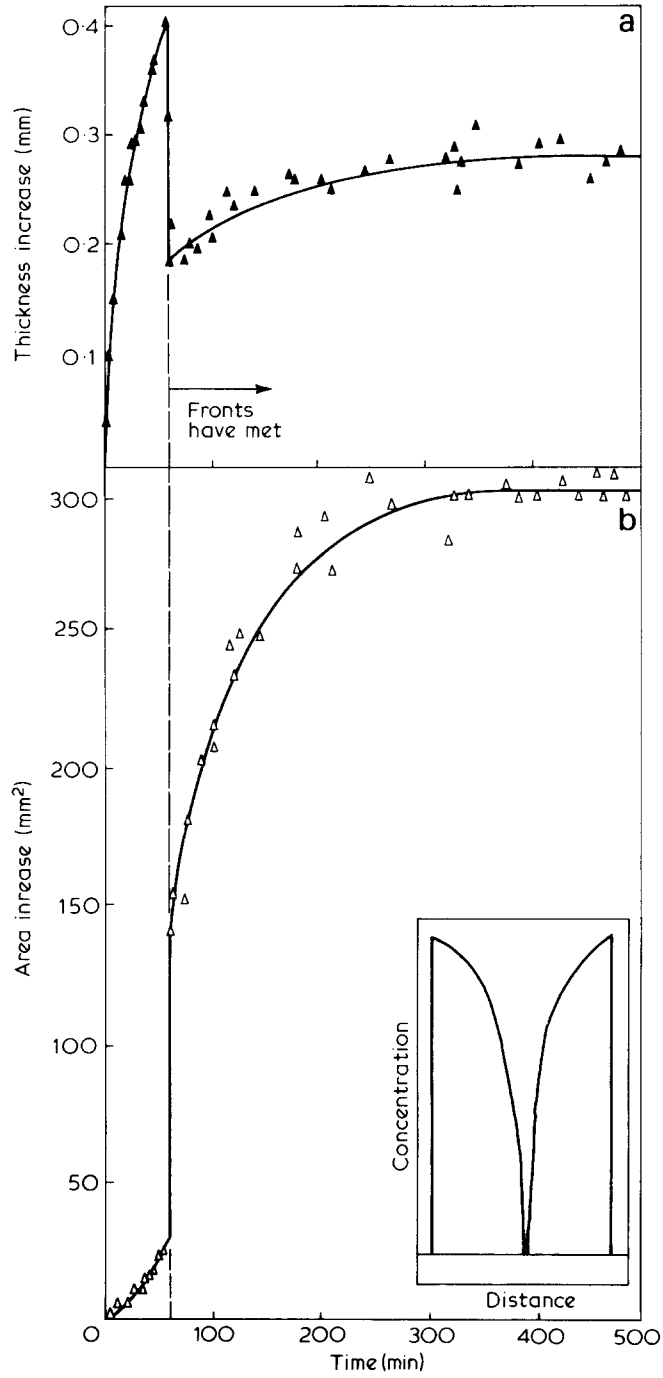

Figure 9 Thickness and area increase as a function of time at 62°C, with inset of concentration profile just before the fronts meet

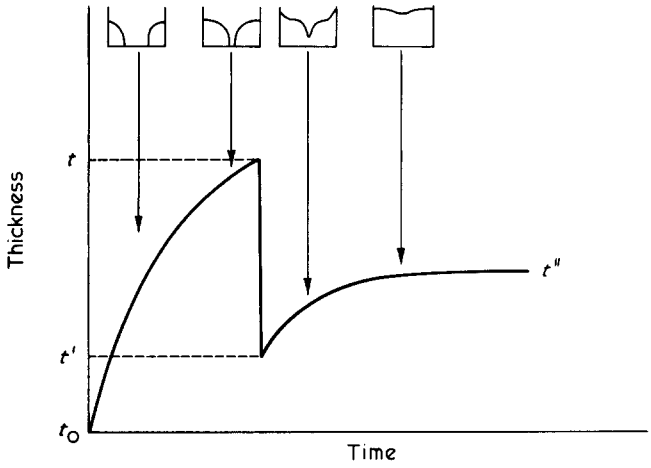

Figure 10 Schematic representation of thickness increase as a function of time at elevated temperatures, with possible concentration profiles shown at various times in the swelling process

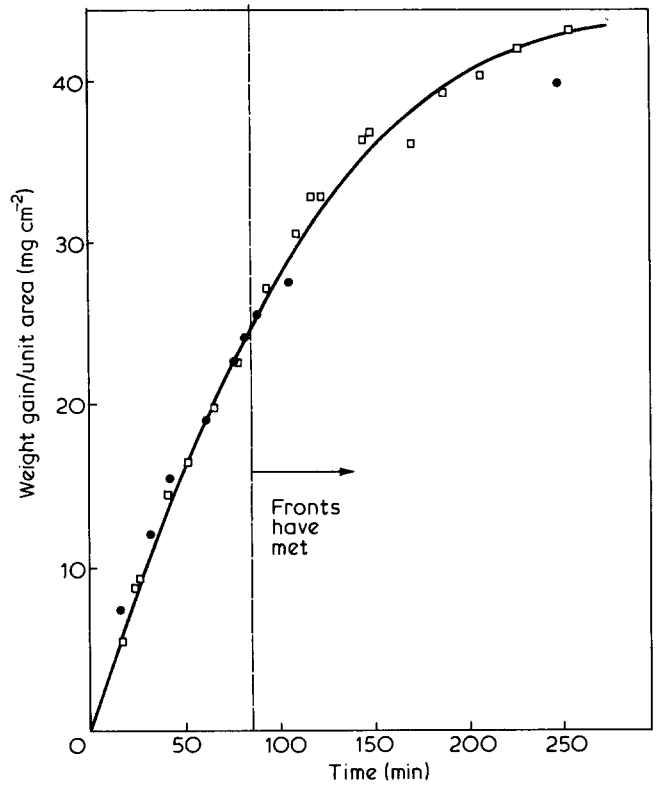

Figure 11 Weight gain/unit area *versus* time, showing: □, experimental points; ●, values derived from measured concentration profiles. Data for 1 mm (nominal) sheet swollen at 52°C (actual average thickness is 0.87 mm)

Prediction of the specimen thickness immediately after shape reversion

The fact that diffusion in the system PMMA–methanol is not pure Case II at elevated temperatures means that a knowledge of the concentration profiles just before the fronts meet is necessary if the change in shape of the specimen on reversion is to be calculated.

For the calculations which follow, the measured profiles are stylized according to *Figure 12* such that the volume fraction of methanol at position x/X is given by equation 12. The values for V_1 and V_2 for the different temperatures are listed in *Table 1*. They are derived from the ratio V_1/V_2 estimated from the actual profiles and the sum $V_1 + V_1/2$ which is related to the measurable parameter t_0/t by equation 14. The volume fraction of liquid v_1 is here defined in the same terms as v_2 so that $v_1 = 1 - v_2$. The fact that it is equated to a measured profile in equation 12, albeit a stylized one, is justified by the experimental observation of the constant ratio between the volume of methanol absorbed and the increase in PMMA volume (c.f. *Figure 2a* and *Figure 2b* in reference 31).

$$v_1\left(\frac{x}{X}\right) = V_1 + V_2.x/X \tag{12}$$

An element i, with volume fraction of methanol v_2, will have swollen to a ratio:

$$(t_0/t)_i = 1 - v_1(i) = 1 - V_1 - V_2.x_i/X \tag{13}$$

Hence the overall swelling just before the fronts meet is given by:

$$t_0/t = \int_0^1 \left[1 - V_1 - V_2.x/X\right] d\left(\frac{x}{X}\right) = 1 - \left(V_1 + \frac{V_2}{2}\right) \tag{14}$$

When the fronts do meet, shape reversion will occur. It is reasonable to assume that, owing to the constraint of its neighbours, each element will decrease in thickness (and thus increase in area) by the same ratio irrespective of the degree to which it has been swollen, and thus will not in general regain its equilibrium shape. Hence the distortion of an element from equilibrium is given by the ratio:

$$\left(\frac{t}{t'}\right)_i = \left(\frac{t}{t_0}\right)_i^{2/3}$$

from equation 3 which can be combined with equation 13 to give:

$$\left(\frac{t}{t'}\right)_i = (1 - v_i)^{-2/3} \tag{15}$$

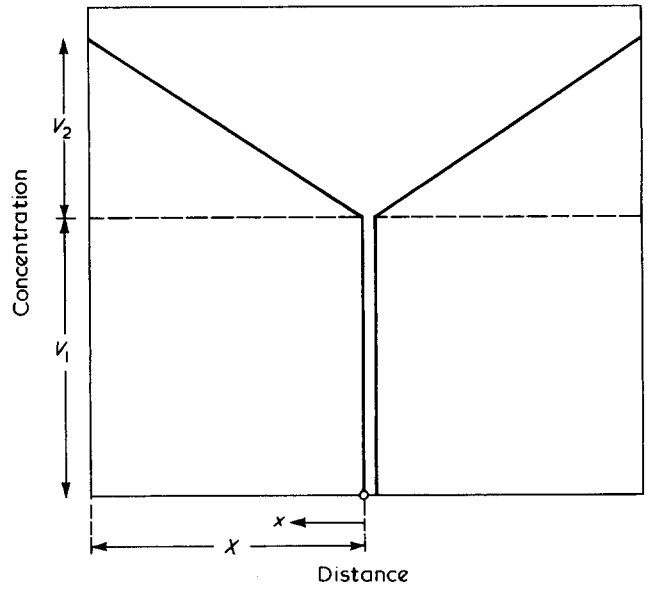

Figure 12 Schematic concentration profile at elevated temperatures as given in equation 12

Table 1 Experimental parameters. (V_1 and V_2 are defined by equation 12, and t_0, t, t' and t'' by *Figures 4* and *10*)

Temperature (°C)	t_0 mm	t mm	t' mm	t'' mm	V_1/V_2	V_1	V_2
24	1.18	1.46	1.35	1.35	∞	0.192	0
42	1.15	1.50	1.29	1.36	3.01	0.198	0.066
52	1.15	1.52	1.31	1.39	1.00	0.164	0.164
62	1.14	1.54	1.31	1.42	0.667	0.148	0.222

Table 2 Comparison of measured and calculated values for the discontinuous shape change

Temperature °C	t/t' measured	ϕ_A (t/t' calc)	ϕ_B (t/t' modulus correction)
24	1.132	1.152	1.152
42	1.163	1.192	1.170
52	1.160	1.213	1.180
62	1.171	1.228	1.186

Owing to constraint the actual relaxation of all elements will be the same at a ratio of $(t/t')_i$ which we style φ_i. Hence the strain ratio in an incompletely relaxed element, expressed with respect to its equilibrium shape, is given by:

$$\frac{t' \text{ actual}}{t' \text{ equilibrium}} = \frac{1}{\varphi_i}(1-v_i)^{-2/3} \tag{16}$$

Now because φ_i is constant for each element, its value will be that which gives elastic stresses in each element which on integration give a net load on the lateral faces of zero. It is possible therefore to calculate a value of φ which should be directly comparable with the experimental ratio t/t'.

Taking the load in an element as

$$P_i = \mathrm{K}\, E_{(i)}\left[\frac{1}{\varphi_i}(1-v_i)^{2/3}-1\right] \tag{17}$$

where K is a constant, $E_{(i)}$ the elastic modulus and the strain ratio of equation 16 has been converted to strain by subtracting unity. We can write:

$$\int_i \mathrm{K}\, E_{(i)}\left[\frac{1}{\varphi_i}(1-v_i)^{2/3}-1\right]\mathrm{d}\left(\frac{x}{X}\right)=0$$

and hence incorporating equation 12 we have:

$$\int_0^1 E\left(\frac{x}{X}\right)\left[\frac{1}{\varphi}(1-V_1-V_2.x/X)^{-2/3}-1\right]\mathrm{d}\left(\frac{x}{X}\right)=0 \tag{18}$$

If we assume for now that the modulus is independent of position then equation 18 gives:

$$\varphi_A = \frac{-3}{V_2}[(1-V_1-V_2)^{1/3}-(1-V_1)^{1/3}] \tag{19}$$

Substitution of the values of V_1 and V_2 listed in *Table 1* gives a series of calculated values of φ_A which is compared directly with the measured ratios t/t' for different temperatures in *Table 2*. The agreement is not particularly good.

Accounting for an elastic modulus (E) *which depends on concentration*

The assumption that the elastic modulus is constant is probably the least justifiable so far. In regions close to the advancing fronts it will, for a given time period, be greater than for nearer the surface. As a first approach we have taken:

$$E = \mathrm{Const}\left[1+Y\left(1-\frac{x}{X}\right)\right] \tag{20}$$

with $Y = C\left(\frac{V_2}{V_1+V_2}\right)$ and C chosen to be 100 so that the ratio of fully swollen to unswollen moduli is typical of that of rubber to glass.

Abbreviating, $(1-V_1)$ as A and $-V_2$ as B the integral,

$$\int_0^1\left[1+Y\left(1-\frac{x}{X}\right)\right]\left[\frac{1}{\varphi_B}\left(1-V_1-\frac{x}{X}V_2\right)^{2/3}-1\right]\mathrm{d}\left(\frac{x}{X}\right).$$

gives when set equal to zero:

$$\varphi_B = \left(\frac{6}{2+Y}\right)\left[\left(\frac{-Y}{4B^2}\right)\left((A+B)^{4/3}-A^{4/3}\right)+\left(\frac{1+Y}{B}+\frac{AY}{B^2}\right)\left((A+B)^{1/3}-A^{1/3}\right)\right]$$

Substitution yields the set of values for the discontinuous change in thickness t/t', listed in the last column of *Table 2*. The agreement is very much better than was obtained when the modulus was assumed constant. No doubt it could be improved further by judicious adjustment of the modulus parameter Y, but such an exercise is somewhat arbitrary and would tell us little. The error bars on the measured values of t/t' have been assessed in the normal way. The calculated values, as they too depend on experimental input (t_0/t and the measured profiles), should also have an assessable error. It is likely to be of the same order as that of the measured t/t'. The lack of agreement at 24°C has already been discussed in the first part of the paper. It is due to the fact that the shape relaxation is relatively slow compared with the diffusivity, and the additional swelling associated with the relaxed state occurs as the specimen is changing shape. At the elevated temperature, however, where the ratio of diffusivity to relaxation rate is less, the shape change appears to be completed before there is any significant increase in the swelling.

In this section we have shown that, on the basis of a knowledge of the increase in specimen thickness and the shape of the concentration profiles just before the fronts meet, it is possible to calculate the discontinuous reduction in thickness as the fronts do meet and the

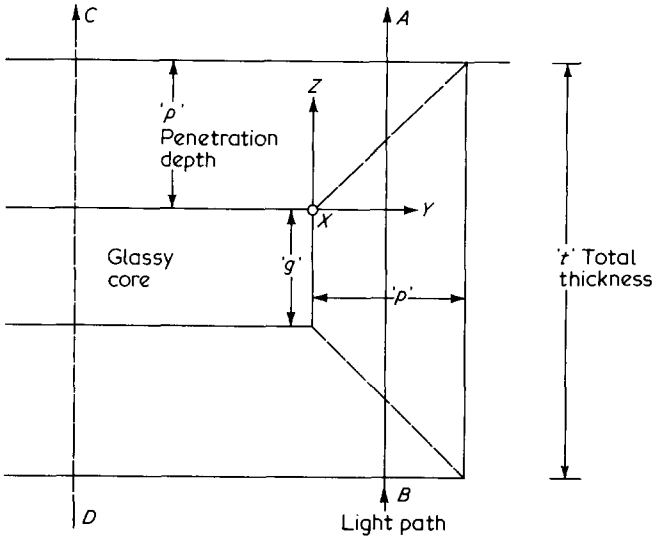

Figure 13 Sectional sketch of specimen showing birefringence geometry. The planar faces of the sheet correspond to the top and bottom of the section

specimen relaxes. These values, which depend on assumptions that the measured profiles can be approximated to a simple geometric form and that the modulus decreases monotonically with increasing concentration, are in reasonable agreement with those measured directly.

ORIENTATION DURING ABSORPTION

Birefringence was observed in the swollen polymer during absorption at 24°C. This optical anisotropy is produced by strains in the swollen layer resulting from the constraining influence of the glassy core.

Figure 13 is a cross-section of a partially swollen specimen showing the direction of the light path (along the z axis), which is perpendicular to the largest face of the specimen. Anisotropy is assumed to be uniaxial with the optic axis perpendicular to the plane of the advancing front, i.e. anisotropy is seen along AB and the material appears isotropic when viewed along CD. This assumption is supported by experimental observation.

The relative retardation (Γ) between two perpendicularly polarized components is related to the birefringence (Δn) by the expression:

$$\Delta n = \frac{\Gamma}{d}$$

where 'd' is the effective distance travelled by the light through the specimen—usually taken as the specimen thickness. In our case, as a first approximation the effective thickness 'd' (i.e. the thickness of anisotropic polymer encountered by light path A–B) is considered to vary linearly between the glassy core thickness 'g' and the total specimen thickness 't' (*Figure 13*). Hence for a partially swollen specimen, if $(p-y)$ is the distance of the light path from the outer edge of the specimen, the value of 'd' is given by simple geometry as: $t-2(p-y)$.

PMMA is an optically negative material[25]. The fast vibration direction can be expected to be parallel to the preferred direction of chain alignment, which is the direction of the tensile stress. Experimental confirmation was obtained that the fast vibration direction in PMMA (both when dry and when swollen in methanol) is parallel to the direction of the applied tensile stress.

Birefringence measurements carried out on sheet specimens of PMMA during swelling in methanol at 24°C showed that the fast vibration direction is perpendicular to the sharp front (and hence the vertical edges of the specimen) i.e. the swollen region is in tension perpendicular to the front and in compression parallel to the front. These observations confirm the explanation of shape change given above—namely that the unswollen glassy core constrains the swollen gel giving rise to compressive stresses in the plane parallel to the swelling fronts and imposing anisotropic volume expansion on the swollen material. Birefringence disappeared after the fronts had met and the specimen had reverted back to its original shape, i.e. when the swelling stresses had been relieved.

The birefringence profile (as a function of distance from the edge surfaces) across the swollen layer in a 3mm sample was measured at successive times and is shown in *Figure 14*. For a given front position, birefringence decreases rapidly with increasing distance behind the front until levelling off at a value of about 1.3×10^{-5}. The shapes of these birefringence profiles are in agreement with those evaluated by Gurnee for the swelling of polystyrene–4% divinylbenzene beads in diethylbenzene[26].

We suggest that the higher values of birefringence immediately behind the front result from the fact that the swelling temperature is in the region of T_g for the swollen phases. The change in shape at the front takes place on a time scale within which the swollen material behaves more as a glass than as a rubber and the birefringence therefore has characteristics of a deformed glass, i.e. it is higher per unit strain than it would be in a rubber[27]. The reduction in birefringence behind the fronts corresponds to the relaxation of a deformed glass to a deformed rubber at constant strain.

STRESSES DEVELOPED ON DESORPTION

Desorption behaviour of fully swollen specimens at 24°C and 62°C was found to differ from that of partially swollen specimens at these temperatures. This is because in the fully swollen state the constraint of the glassy core

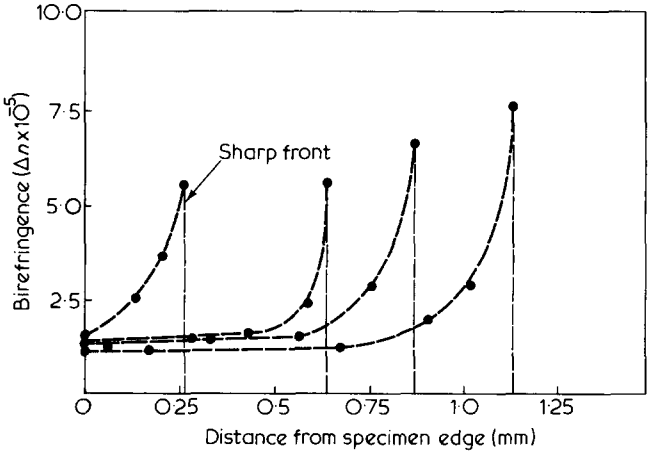

Figure 14 Birefringence profiles in a 3 mm thick sample of PMMA swollen in methanol at 24°C. The distances from the edge surface of the specimen are in the minus y direction (c.f. *Figure 13*)

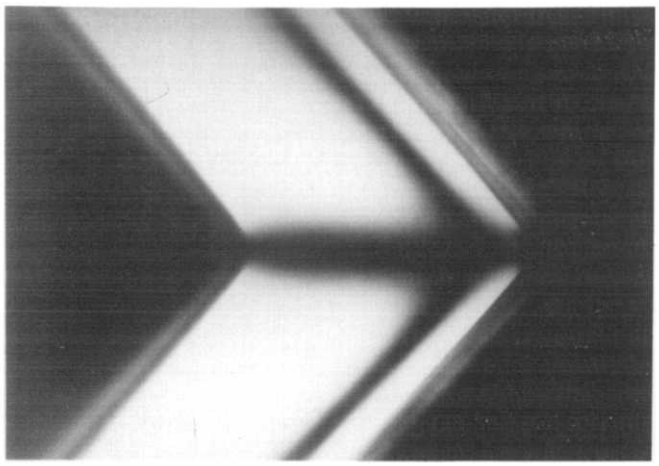

Figure 15 Specimen photographed between crossed polars, showing the development of tensile stress parallel to the surfaces during desorption. (Photographed 15 min after removal of specimen from the solvent bath.)— see text

has been lost and the swollen gel is able to relax to relieve the deformation introduced by the shape change on swelling—as is evident from the disappearance of swelling birefringence. Hence a fully swollen sample is essentially a stress-free rubber, whereas the swollen region in a partially swollen specimen behaves as a deformed rubber.

On removal of a completely swollen specimen from the solvent bath, the specimen rapidly loses methanol from its surfaces and so initial desorption rates are high. The process of penetrant desorption from a plasticized rubber is expected to have Fickian characteristics. However, as the surface layers become depleted of solvent, the rate of diffusion drops off because the diffusion coefficient, D, is strongly dependent (probably exponentially) on concentration. At a certain solvent concentration the surface layers may be regarded to change from a swollen rubber to a swollen glass, giving a depleted layer acting as a skin. On losing solvent the surface layers tend to contract but are constrained by the inner swollen gel, so that tensile stresses tend to develop in the surface region: hence the idea of a skin stretched over a compressed gel[28]. In 1mm PMMA sheet specimens, however, birefringence measurements revealed that these tensile stresses are only of the order of a few MNm^{-2} and they decay as desorption proceeds so that an almost completely desorbed specimen has negligible birefringence.

During desorption of partially swollen specimens, the birefringence in the swollen region is observed to change sign and increase greatly in magnitude. As methanol is lost from the surface layers they contract, and because of the constraint of the glassy core, change shape so as to retain constant area. However when a proportion of the methanol has been lost the T_g of the surface layers will increase above ambient and they will become glassy. They will however still lose methanol, albeit at a much reduced rate, and this further contraction endeavours to occur without change of shape which is difficult for a glass. The constraint of the glassy core opposes isotropic contraction, with the result that biaxial tensile stresses develop parallel to the surface and thus normal to the extension direction of the previously swollen surface layers. The elastic-birefringent response of these layers, which for PMMA is both stronger than that derived from the molecular orientation in a deformed rubber and of the same sign, means that the observed birefringence changes sign. In white light a zero-order-fringe marks the position where the birefringence due to the remaining molecular extension normal to the surface (introduced as the surface layers swelled) is exactly compensated by the birefringence resulting from the biaxial elastic extension of the glass in the plane of the surface. This is shown in *Figure 15*. As desorption proceeds this fringe moves inwards, until the birefringence in the whole penetrated region is dominated by the component due to biaxial tension on the glassy material.

On desorption of partially swollen specimens, the whole of the swollen layer is soon in a state of biaxial tension. Birefringence measurements of the elastic stress in the unpenetrated core confirm that the tension in the swollen shell is balanced by compressive stresses in the core. The magnitude of the tensile stress developed on desorption was found to depend on the degree (and hence temperature) of swelling and the thickness of the swollen layer: the greater the degree of swelling and the smaller the thickness of the swollen layer, the higher the tensile stresses developed.

The build up of tensile stresses in the surface of a specimen swollen for 25 h at 24°C and allowed to desorb, is shown in *Figure 16*. The stress optical coefficient of unplasticized PMMA in uniaxial tension (that is 3.3×10^{-12} m^2 N^{-1})[29] was used to calculate stress from the measured values of birefringence. This value of the stress optical coefficient may be a little low for this situation because the stress optical coefficient (in plane strain compression) in a specimen of PMMA fully swollen in methanol at 24°C was found to be $8 \times 10^{-12} m^2 N^{-1}$, and presumably there is residual methanol at the surface of the desorbing specimen. The tensile stress attained in the specimen surface (i.e. 75 MNm^{-2}) is surprisingly large and approaches the yield stress of PMMA.

On desorption, very high tensile stresses can develop in the surfaces of specimens swollen for short periods of time at 62°C (*Figure 17*). Values as high as 150 MNm^{-2} have been estimated using the stress optical coefficient of unplasticized PMMA mentioned above. Although such values may seem unreasonably high, the biaxial tension in

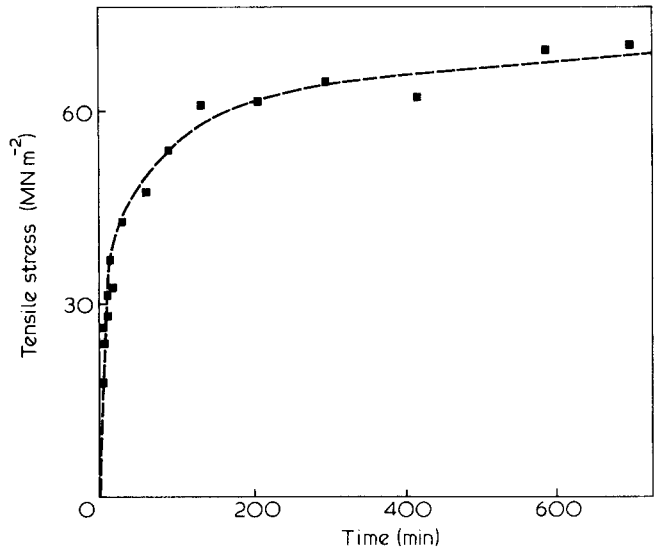

Figure 16 Development of desorption stress at the specimen edge, for 1 mm PMMA sheet swollen in methanol at 24°C for 25 h

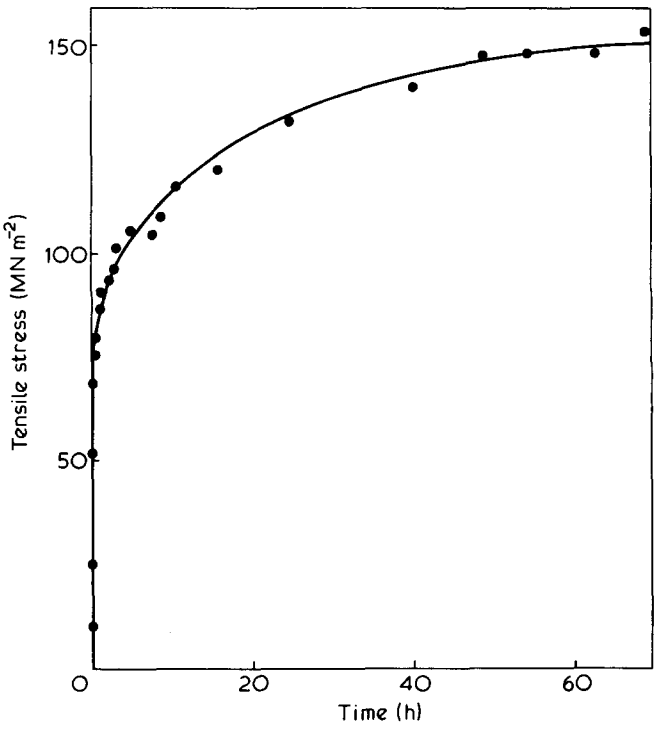

Figure 17 Build up of tensile stress at the specimen surface during desorption after swelling 1 mm PMMA sheet for 5 min at 62°C

the specimen surface is certainly high enough to initiate crazing, as shown for example in *Figures 18(a)* and *(b)*. The development of crazes did not occur immediately on removal of specimens from the methanol bath, but in fact took place slowly over a period of several weeks. It is not clear whether the methanol in the swollen region plays any specific part in the craze formation process, since the tensile stresses developed in the specimen are quite high enough to initiate craze formation in PMMA in air. For example, Williams *et al.*[30] have reported a craze initiation stress for unnotched PMMA specimens in air (loaded at an extension rate of 0.5 cm min^{-1}) of 67.8 MNm^{-2}.

The fissures produced in the specimen surface on desorption heal up when the specimen is reimmersed in methanol and allowed to swell to an equilibrium state. This suggests that they are more likely to be crazes than cracks.

Further birefringence measurements were made on a series of specimens which had been partially swollen at temperatures between 42°C and 62°C and allowed to desorb in air for up to 16 months. It was assumed that after this period of time there would be very little residual methanol in the surface layers of the specimens. A definite correlation was observed between birefringence and the thickness of the swollen layer, as shown in *Figure 19*, i.e. higher tensile stresses are developed on desorption for smaller penetration depths. This presumably results from the higher constraint and the relatively higher rates of desorption: the former keeping the surface area rigidly fixed and the latter causing a rapid rubber to glass transition and preventing the polymer depleted in methanol from returning to its original shape. The specimens which were found to have crazed were those with a birefringence greater than 30×10^{-5}, i.e. with tensile stresses in the swollen region greater than 90 MNm^{-2}.

In view of the high tensile stresses observed during desorption of partially swollen specimens, it is not surprising that crazes develop on reimmersion, because the craze initiation stress for PMMA in methanol is only about 21 MNm^{-2} [30]. By carrying out a series of absorption–desorption cycles it is possible to produce a network of well-developed crazes in the swollen region, which leads to fracture when the penetrating solvent fronts meet at the centre of the specimen.

CONCLUSIONS

(i) Specimens of PMMA immersed in methanol were found to change shape during swelling. The unpenetrated glassy core imposes a constraint on the swollen gel and all volume expansion appears as an increase in thickness. When the sharp fronts, separating swollen and unpenetrated regions, meet at the centre of the specimen the constraint of the glassy core is relieved and the samples increase in area and decrease in thickness tending to revert to their original shape. This reversion of shape change does not occur at constant volume: a comparison of estimated volumes before and after the fronts meet revealed that there is an increase in volume accompanying the relief of compressive stresses on the swollen gel. This phenomenon, i.e. increased imbition accompanying the release of stress is predicted by the thermodynamic theory of the deformation of swollen networks.

At elevated temperatures there is a concentration gradient across the swollen gel so that the swelling and shape reversion processes are more complex than at ambient temperatures, when the concentration profile can

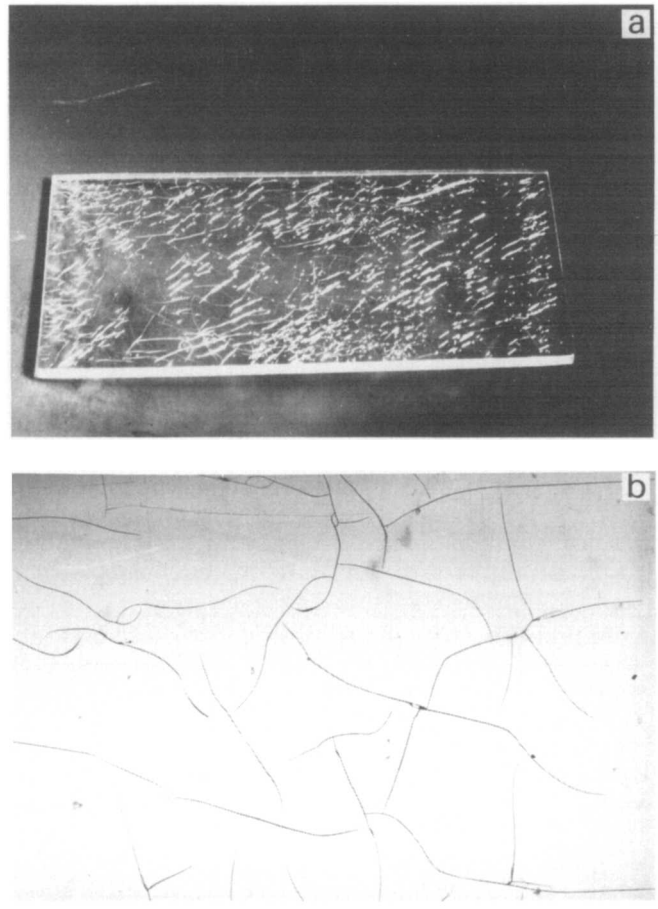

Figure 18 Craze formation on desorption in a specimen swollen at 64°C. (a) Magnification x 3.3 (b) Magnification x 40

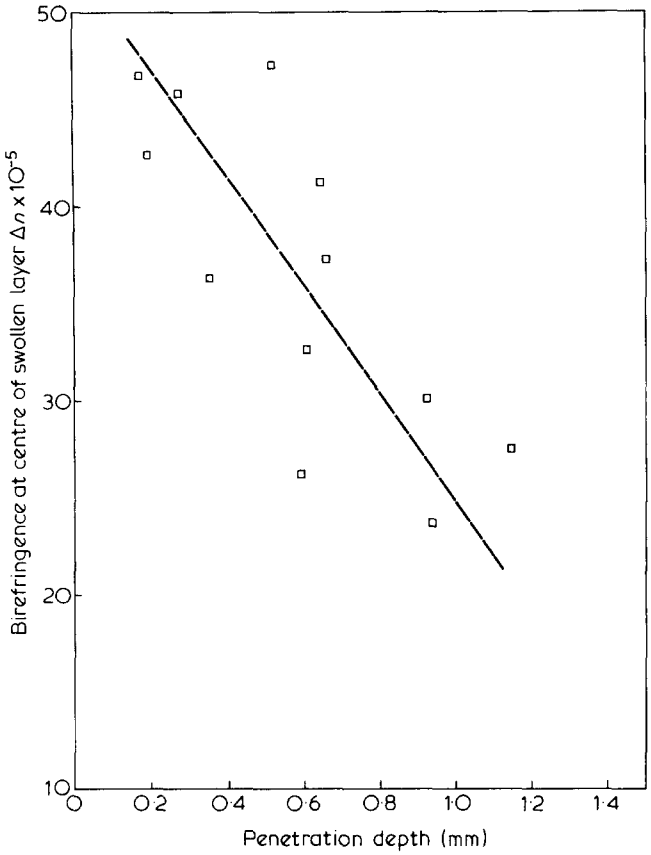

Figure 19 Relationship between birefringence and penetration depth. Specimens were partially swollen at temperatures between 42° and 62°C and allowed to desorb for up to 16 months

be represented by a simple step function. Swelling is an 'averaging' process at elevated temperatures, but with simple modelling of concentration profiles and the dependence of modulus on concentration it has been possible to estimate the strains produced during the shape change process and get reasonable agreement with experimental values.

At ambient temperatures the swollen gel is effectively at its T_g and so when the fronts meet the specimen very slowly relaxes until it has completely returned to its original shape. At higher temperature the swollen gel is rubbery. Reversal of shape change begins to occur immediately when the fronts meet, but some stress relaxation has occurred and even at equilibrium swelling the specimens have not returned completely to their original shape.

(ii) Partially swollen specimens exhibited birefringence. The slow vibration direction is parallel to the sharp front, indicating that the swollen region is in compression in the plane parallel to the front and in tension perpendicular to the front. The sign of the birefringence on swelling is therefore compatible with chain orientation parallel to the direction of diffusion. The birefringence profile reveals high values in the swollen polymer just behind the front which drop to a lower constant value in the region remote from the front. The reduction in birefringence behind the front is accounted for by the relaxation of the swollen glass to a deformed rubber at constant strain.

(iii) A study of desorption behaviour in the PMMA/methanol system revealed that even short exposure to a swelling medium may cause damage to a polymer sample by the introduction of high tensile stresses into its surface on desorption. The tensile stresses, revealed by birefringence measurements, are of the order of the yield stress of the PMMA and well above the initiation stress for solvent crazing in methanol. These tensile stress levels are sufficient to cause limited air crazing in PMMA and pronounced crazing on re-immersion in the solvent. A series of sorption-desorption cycles can produce substantial mechanical damage.

It is thus possible by partial sorption followed by desorption to generate mechanical damage without the application of any external stress, or the presence of any internal stress in the original material.

REFERENCES

1 Treloar, L. R. G. 'The Physics of rubber elasticity', Clarendon 1975, p 154
2 Flory, P. J. 'Principles of polymer chemistry', Cornell, 1953, 576
3 Smith, K. J., from Jenkins, A. D. 'Theories of Chain coiling, Elasticity and Viscoelasticity' Volume 1, North Holland 1973, p 372
4 Dreschel, P., Hoard, J. L. and Long, F. A. *J. Poly. Sci.* 1953, **10**, 241
5 Park, G. S. *J. Poly. Sci.* 1953, **11**, 97
6 Alfrey, T., Gurnee, E. F. and Lloyd, W. G. *J. Polym. Sci.* (C) 1966, **12**, 249
7 Hopfenberg, H. B., Holley, R. H. and Stannet, V. *Polym. Eng. Sci.* 1969, **9**, 242
8 Thomas, N. L. and Windle, A. H. *Polymer* 1978, **19**, 255
9 Hopfenberg, H. B., Nicolais, L. and Drioli, E. *Polymer* 1976, **17**, 195
10 Kwei, T. K. and Zupko, H. M. *J. Polym. Sci. (A2)* 1969, **7**, 867
11 Hartley, G. S. *Trans. Faraday Soc.* 1949, **45**, 820
12 Crank, J. *Trans. Faraday Soc.* 1951, **47**, 450
13 Hermans, P. H. 'A Contribution to the physics of cellulose fibres' Elsevier 1948, New York–Amsterdam p 23
14 Rosen, B. *J. Poly. Sci.* 1960, **47**, 525
15 Michaels, A. S., Bixler, H. J. and Hopfenberg, H. B. *J. Appl. Poly. Sci.* 1968, **12**, 991
16 Hopfenberg, H. B., Holley, R. H. and Stannet, V. T. *Poly. Eng. & Sci.* 1970, **10**, 376
17 Thomas, N. L. and Windle, A. H. *Polymer* 1980, **21**, 613
18 Flory, P. J. and Rehner, J. *J. Chem. Phys.* 1943, **11**, 521
19 Hermans, J. J. *Trans. Faraday Society* 1947, **43**, 591
20 Flory, P. J. *J. Chem. Phys.* 1950, **18**, 108
21 Hermans, J. J. *J. Poly. Sci.* 1962, **59**, 191
22 Flory, P. J. *Proc. Roy. Soc.* 1976, **351**, 351
23 Brown, H. R. *Polymer* 1978, **19**, 1186
24 Jacques, C. H. M., Hopfenberg, H. B. and Stannett, V. 'Permeability of Plastic Films and Coatings' 1974 (Ed. H. B. Hopfenberg), Plenum Press, New York, p 73
25 Robinson, H. A., Ruggy, R. and Slantz, E. *J. Appl. Phys.* 1944, **15**, 343
26 Gurnee, E. F. *J. Poly. Sci.* 1959, **41**, 119
27 Pick, M., Lovell, R. and Windle, A. H. *Polymer* 1980, **21**, 1019
28 Downes, J. G. and McKay, B. H. *J. Poly. Sci.* 1959, **36**, 130
29 Read, B. E. *J. Poly. Sci. C*, 1967, **16**, 1887
30 Williams, J. G., Marshall, G. P., Graham, I. and Zichy, E. L. 'Pure and Applied Chemistry' 1974, **39**, 275
31 Thomas, N. L. and Windle A. H. *Polymer* 1977, **18**, 1195